Inorganic Chemistry
Cite This: Inorg. Chem. XXXX, XXX, XXX−XXX
Communication
pubs.acs.org/IC

An Ultrasensitive and Selective Metal−Organic Framework Chemosensor for Palladium Detection in Water

Aasif Helal,*[,†] Ha L. Nguyen,[†,‡] Amir Al-Ahmed,[§] Kyle E. Cordova,[†,‡] and Zain H. Yamani[†]

[†]Center of Research Excellence in Nanotechnology and [§]Center of Research Excellence in Renewable Energy, King Fahd University of Petroleum and Minerals, Dhahran 31261, Saudi Arabia

[‡]Department of Chemistry and Berkeley Global Science Institute, University of California, Berkeley, Berkeley, California 94720, United States

Supporting Information

ABSTRACT: A new europium-based metal−organic framework, termed KFUPM-3, was constructed using an allyloxy-functionalized linker. As a result of coordinative interactions between the allyloxy moieties and Pd^{2+}, highly selective changes in both the absorption and emission spectra of KFUPM-3 were observed. Accordingly, KFUPM-3 was demonstrated to have an ultrasensitive Pd^{2+} detection limit (44 ppb), regenerative properties without loss in performance, detection of palladium in different oxidation states and in the presence of other competitor metal ions, and fully functional sensing capabilities over a wide pH range.

In the design of new chemosensors for palladium detection, there are five criteria that must be met: (i) high-intensity fluorescence; (ii) selectivity for palladium over other potential contaminants; (iii) ability to operate with a low detection limit; (iv) reversibility such that the chemosensor can be regenerated; (v) stability in aqueous media under different pH conditions.[1] Considering these criteria, metal−organic frameworks (MOFs) are attractive in that their constituent building blocks can be designed and functionalized in a rational manner.[2−5] Specifically, MOFs constructed from lanthanide-containing secondary building units (SBUs) are ideal especially when stitched together by organic linkers with fluorogenic properties.[6] In this way, direct energy transfer from appropriately designed organic linkers in their excited state to the lanthanide SBUs results in "luminescence sensitization".[7] Furthermore, the organic linkers can be functionalized with moieties that selectively and reversibly interact with palladium, even in environments where low concentrations are present.[8,9] This allows for the MOF backbone to be equipped with both recognition of palladium via coordinative binding and a fluorogenic site that correspondingly responds to this binding. Although MOFs have been designed with pyridinyl donors that effectively coordinate palladium, alkene functional groups are better suited because of their π-donor capabilities, which allow for selective and reversible coordination.[10−14]

Herein, we report the design and synthesis of a new MOF chemosensor that meets the aforementioned criteria for palladium detection. Our strategy focused on the construction of a MOF using Eu^{3+} to form the SBUs, which then were stitched together by organic linkers that integrated allyloxy moieties to ensure a selective and reversible recognition site for palladium. Through a facile solvothermal synthesis, the resulting MOF, termed KFUPM-3, was highly crystalline, and structural analysis revealed a two-dimensional **sql** topology. As expected, highly selective changes in both the absorption and emission spectra of KFUPM-3 were confirmed upon exposure to aqueous solutions containing palladium at various concentrations. Furthermore, it was demonstrated that KFUPM-3 had an ultrasensitive Pd^{2+} detection limit of 44 ppb, demonstrated regenerative properties, was capable of selectively detecting palladium in different oxidation states and in the presence of other heavy metal ions, and operated over a wide pH range.

The first step in realizing a new MOF chemosensor centered on the design of a linker that was capable of selectively binding palladium. After protecting the carboxylic acid of the commercially available 2,5-dihydroxyterephthalic acid, we performed a Williamson ether synthesis to introduce allyloxy groups at the 2 and 5 positions of the terephthalic acid (see sections S1 and S2). This was followed by a saponification to deprotect the allyloxy-functionalized linker in order to achieve the targeted 2,5-bis(allyloxy)terephthalic acid (H_2BAT) in 85% yield. The synthesized H_2BAT was fully characterized by NMR (^1H and ^{13}C) and elemental analysis (see section S2). With H_2BAT in hand, MOF synthesis was then performed under solvothermal conditions. Specifically, $Eu(NO_3)_3{\cdot}5H_2O$ and H_2BAT were dissolved in a 5:2:1 (v/v) solution of *N*,*N*′-dimethylformamide (DMF), ethanol, and water, respectively, and the resulting solution was heated at 80 °C for 3 days to produce KFUPM-3 as colorless, rhombohedral-shaped single crystals (see section S2).

Single-crystal X-ray diffraction analysis revealed that KFUPM-3 crystallized in the $P\bar{1}$ (No. 2) space group with unit cell parameters of a = 18.07 Å, b = 18.98 Å, c = 22.53 Å, α = 106.8°, β = 113.3°, and γ = 96.9° (Figure 1a,b and section S2 and Table S1). Through structural analysis, it was evident that the europium-based SBU contained two crystallographically independent Eu atoms, which are linked together by a μ_3-O originating from a carboxylate of the BAT^{2-} linker. Each Eu atom adopts a tricapped trigonal-prismatic geometry from the coordination of eight carboxylates and one DMF guest molecule. The dinuclear Eu−O SBU is surrounded by six BAT^{2-} linking units, in which the directionality of these linkers

Received: October 11, 2018

DOI: 10.1021/acs.inorgchem.8b02871
Inorg. Chem. XXXX, XXX, XXX−XXX

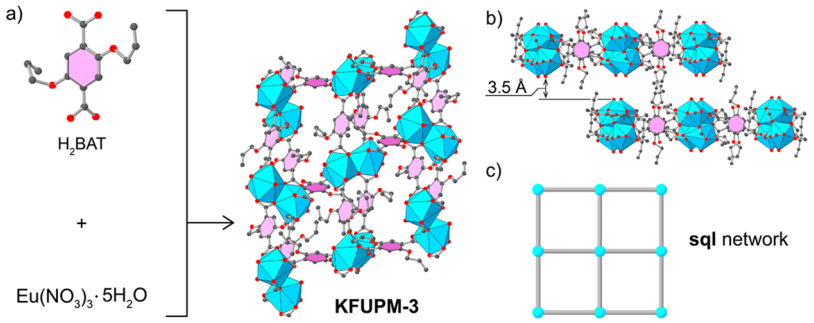

Figure 1. (a and b) Single-crystal structure of KFUPM-3 constructed from H_2BAT and Eu^{3+} building blocks. (c) Structure of KFUPM-3, which adopts a two-dimensional-layered sql network. Atom colors: Eu, blue polyhedral; C, gray; O, red. H atoms are omitted for clarity.

can be reduced to four total points of extension. As a result, the structure is extended in two dimensions, adopts the **sql** topology with a 4^4 tiling (Figure 1c), and has square-shaped pore windows of ∼4 Å size. Because of van der Waals forces, the interlayer spacing of KFUPM-3 is ∼3.5 Å.

After solvent exchange and activation, powder X-ray diffraction (PXRD) analysis confirmed phase purity upon a comparison of the experimental diffraction patterns and the diffraction pattern simulated from the single-crystal structure (see section S3). Fourier transform infrared spectroscopy measurements for KFUPM-3 demonstrated the presence of the characteristic stretching vibrational bands of the allyloxy moiety as well as shifted absorption bands for the carboxylate moiety upon coordination (see section S3). The thermal stability of KFUPM-3 was proven via thermal gravimetric analysis, in which two main weight losses were observed: (i) 8 wt % in the temperature range of 200−300 °C, which was assigned to the loss of coordinated DMF and water within the pores; (ii) 58 wt % in the temperature range of 300−800 °C, which was assigned to framework decomposition. The remaining residue (34 wt %) was attributed to Eu_2O_3 (see section S3). A N_2 adsorption isotherm at 77 K revealed that KFUPM-3 was microporous with a Brunauer−Emmett−Teller surface area of 227 $m^2\ g^{-1}$ and a pore volume of 0.159 $cm^3\ g^{-1}$ (see section S3). Scanning electron microscopy images display a crystal morphology of flat rectangular sheets varying from 10 to 15 μm in size (see section S3).

After a successful structural characterization, we turned our attention to investigating the photophysical properties of KFUPM-3 (see section S4). As such, the UV−vis absorption spectrum for KFUPM-3 displayed two peaks, centered at 252 and 336 nm, which resulted from $\pi-\pi^*$ transitions of the benzene ring and allylic bond. Optical sensing measurements were then performed using 10^{-2} M aqueous solutions of Pd^{2+}. Upon the slow addition of Pd^{2+} to a suspension of KFUPM-3, the absorbance increased and an additional peak, centered at 276 nm, was observed (see section S4). This new peak suggested that a possible coordinative interaction was occurring between Pd^{2+} and the allyloxy moiety of KFUPM-3. This response was found to be highly selective because no such changes were observed when other metal ions (e.g., Na^+, K^+, Ca^{2+}, Mg^{2+}, Sr^{2+}, Rb^+, Cs^+, Fe^{2+}, Fe^{3+}, Co^{2+}, Cu^{2+}, Ni^{2+}, Zn^{2+}, Cd^{2+}, Ag^+, Al^{3+}, Ga^{3+}, Ir^{3+}, Rh^{3+}, Pt^{2+}, and Pb^{2+}) were tested. The stoichiometry of the binding event was then verified by Job's method, which concluded that a 1:2 stoichiometric complex was formed between KFUPM-3 and Pd^{2+}, respectively (see section S4).[8,9] It is worth noting that the crystallinity of KFUPM-3, as proven by PXRD analysis, was retained after the binding event with Pd^{2+} took place (see section S3). Fluorescence spectroscopy measurements were then carried out at an excitation wavelength of 336 nm (see section S5). At 336 nm, energy transfer occurs from the BAT^{2-} linker excited states to the ground state of the Eu^{3+} ions, with fluorescence emissions resulting from f−f transitions. Emission peaks were observed at 578, 592, 616, 648, and 695 nm, which correspond to $^5D_0 \rightarrow {}^7F_0$, $^5D_0 \rightarrow {}^7F_1$, $^5D_0 \rightarrow {}^7F_2$, $^5D_0 \rightarrow {}^7F_3$, and $^5D_0 \rightarrow {}^7F_4$ transitions, respectively (Figure 2).[12,13] The most intense fluorescent peak is the $^5D_0 \rightarrow {}^7F_2$

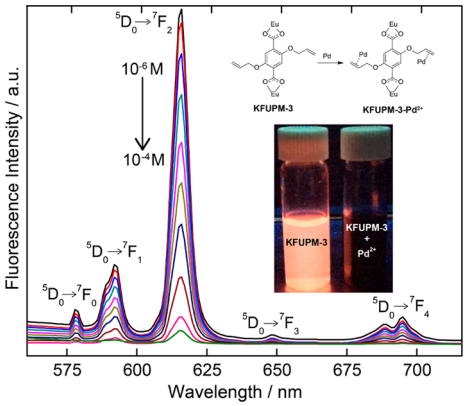

Figure 2. Changes in the emission spectrum of KFUPM-3 in water upon the incremental addition of $PdCl_2$ in water (λ_{ex}= 336 nm). Inset: Mechanism of palladium binding and fluorogenic change from orange (KFUPM-3) to colorless (KFUPM-3-Pd^{2+}) upon the addition of Pd^{2+} (λ_{ex} = 336 nm).

transition originating from an Eu^{3+} ion with anti-inversion symmetry.[15,16] It is also noted that emission of the BAT^{2-} linker does not appear in the emission spectrum of KFUPM-3, which indicates that an antenna effect is present. Finally, the absolute quantum yield for KFUPM-3 was calculated from the integrated sphere to be 0.48, and the CIE coordinates, obtained from the chromaticity diagram, agree with the experimentally derived emission results (see section S5).

In order to understand the sensitivity of the chemosensing properties of KFUPM-3, changes to the fluorescence emission intensity were investigated as a function of increasing Pd^{2+} concentration. As expected, fluorescence was quantitatively quenched upon exposure to increasing concentrations of Pd^{2+} and observed to be completely quenched when a 2:1 Pd^{2+}/KFUPM-3 molar ratio was achieved. This complete quenching indicates that full complexation was realized between Pd^{2+} and the two allyloxy moieties on the BAT^{2-} linker (Figure 2) because of the strong interaction between the π−d orbital of

DOI: 10.1021/acs.inorgchem.8b02871
Inorg. Chem. XXXX, XXX, XXX−XXX

alkene and palladium. It is noted that Pd^{2+} complexation within the channels of KFUPM-3 perturbs the electronic structure of the BAT^{2-} linker, which affects the excited state of the linkers. This perturbation then impacts sensitization of the Eu^{3+} emissive state by prohibiting energy transfer from the linkers to the Eu^{3+} SBUs, which, consequently leads to quenching of fluorescence. The quenching efficiency was then interpreted by calculating the Stern−Volmer constant.[8,9] On the basis of the titration curve, shown in Figure 2, the Stern−Volmer constant, K_{SV}, was calculated to be 7.8×10^4, which is comparable to values obtained for other suspension-based Pd^{2+} chemosensors (see section S5). The sensitivity of KFUPM-3 toward Pd^{2+} was demonstrated based on the calculated detection limit. For KFUPM-3, this detection limit was 44 ppb, which is significantly lower than the 5−10 ppm threshold for palladium in pharmaceutical products (see section S5).[17] Furthermore, this detection limit is among the lowest and most sensitive reported for MOF-based Pd^{2+} chemosensing materials (Table S2). To assess changes in the emission spectra in the presence of metal contaminants, KFUPM-3 was again immersed in solutions of different metal ions (see section S5). As shown in Figure 3, the

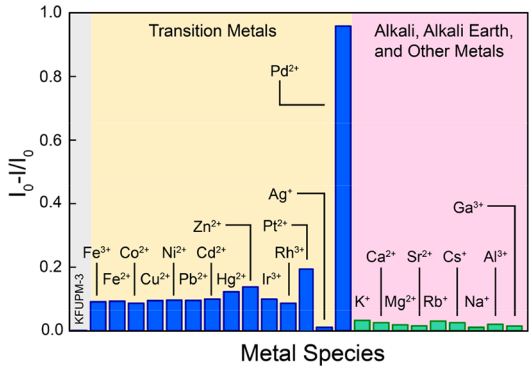

Figure 3. Change in the normalized fluorescence emission of KFUPM-3 in water upon the addition of 200 μL of different metal cations (10^{-2} M; λ_{ex} = 336 nm).

emission remained for all metal ions tested, whereas the emission was quenched when Pd^{2+} was in the presence of KFUPM-3. Again, this demonstrates that a highly selective chemosensing process is occurring for KFUPM-3 with Pd^{2+}.

Competition experiments were then carried out in order to explore the possibility of using KFUPM-3 as a practical ion-selective (Pd^{2+}) fluorescent chemosensor. In these studies, KFUPM-3 was first exposed to 200 μL of various competitor metal ions (10^{-2} M), at which time 200 μL of Pd^{2+} was then added. Fluorescence emission spectroscopy exhibited no interference in the emission when competitor metal ions were present with Pd^{2+} (see section S5). For environmental and physiological applications, chemosensors also must operate in media with widely varying pHs. The emission properties and crystallinity of KFUPM-3 were effectively maintained within a pH range of 6.0−10.0 (see section S6). Beyond this range, the structure of KFUPM-3 decomposes, as proven by PXRD analysis, and the emission properties are lost (see section S6). The emission response of KFUPM-3 was also evaluated in the presence of different palladium species with varying oxidation states: $PdCl_2$, $Pd(PPh_3)_4$, $Pd(OAc)_2$, $PdCl_2(PPh_3)_2$, $(NH_4)_2PdCl_6$, and $Pd_2(dba)_3$ in deoxygenated water and acetonitrile. As such, negligible differences were observed for the emission response of KFUPM-3 toward these differing palladium species. Because no additional reagents were added during the analysis to alter the oxidation states of these species, it is presumed that KFUPM-3 can interact with palladium irrespective of the oxidation state (see section S7).

Finally, the reusability of KFUPM-3 as a practical chemosensor was demonstrated. In a typical experiment, dispersion of KFUPM-3-Pd^{2+} (KFUPM was pre-exposed to Pd^{2+}) in aqueous media was treated with 0.1 M ethylenediaminetetraacetic acid. Fluorescence spectroscopy was then performed, and an emission signal, with a maximum at 616 nm, was observed to be recovered over the course of four consecutive cycles. This study powerfully demonstrates that KFUPM-3-Pd^{2+} coordinative binding is chemically reversible as opposed to an irreversible cation-catalyzed reaction (see section S8). Moreover, the diffraction pattern of KFUPM-3 showed that the crystallinity of the material was maintained (see section S8).

■ ASSOCIATED CONTENT

Supporting Information

The Supporting Information is available free of charge on the ACS Publications website at DOI: 10.1021/acs.inorgchem.8b02871.

Linker synthesis and characterization, full KFUPM-3 synthetic details and characterization, and experimental conditions for sensing measurements (PDF)

Accession Codes

CCDC 1870943 contains the supplementary crystallographic data for this paper. These data can be obtained free of charge via www.ccdc.cam.ac.uk/data_request/cif, or by emailing data_request@ccdc.cam.ac.uk, or by contacting The Cambridge Crystallographic Data Centre, 12 Union Road, Cambridge CB2 1EZ, UK; fax: +44 1223 336033.

■ AUTHOR INFORMATION

Corresponding Author

*E-mail: aasifh@kfupm.edu.sa (A.H.).

ORCID

Ha L. Nguyen: 0000-0002-4977-925X
Kyle E. Cordova: 0000-0002-4988-0497
Zain H. Yamani: 0000-0002-6031-9385

Author Contributions

The manuscript was written through contributions of all authors.

Notes

The authors declare no competing financial interest.

■ ACKNOWLEDGMENTS

We acknowledge Prof. Omar M. Yaghi (University of California, Berkeley) for continued support. We acknowledge Profs. Enrique Gutierrez-Puebla and Angeles Monge Bravo (Instituto de Ciencia de Materiales de Madrid, Spain) for a productive discussion in the single-crystal structure solution. We are grateful to Saudi Aramco for supporting the MOF synthesis and characterization (Grant ORCP2390). The sensing studies were supported by King Abdulaziz City for Science and Technology, National Science, Technology, and Innovation Plan (Grant 15-NAN4601-04).

DOI: 10.1021/acs.inorgchem.8b02871
Inorg. Chem. XXXX, XXX, XXX−XXX

REFERENCES

(1) Tracey, M. P.; Pham, D.; Koide, K. Fluorometric Imaging Methods for Palladium and Platinum and the Use of Palladium for Imaging Biomolecules. *Chem. Soc. Rev.* **2015**, *44*, 4769−4791.

(2) Furukawa, H.; Cordova, K. E.; O'Keeffe, M.; Yaghi, O. M. The Chemistry and Applications of Metal-Organic Frameworks. *Science* **2013**, *341*, 1230444.

(3) Lin, X.; Gao, G.; Zheng, L.; Chi, Y.; Chen, G. Encapsulation of Strongly Fluorescent Carbon Quantum Dots in Metal−Organic Frameworks for Enhancing Chemical Sensing. *Anal. Chem.* **2014**, *86*, 1223−1228.

(4) Lin, X.; Luo, F.; Zheng, L.; Gao, G.; Chi, Y. Fast, Sensitive, and Selective Ion-Triggered Disassembly and Release Based on Tris-(bipyridine)Ruthenium(II)-Functionalized Metal− Organic Frameworks. *Anal. Chem.* **2015**, *87*, 4864−4870.

(5) Luo, F.; Lin, Y.; Zheng, L.; Lin, X.; Chi, Y. Encapsulation of Hemin in Metal−Organic Frameworks for Catalyzing the Chemiluminescence Reaction of the H_2O_2−Luminol System and Detecting Glucose in the Neutral Condition. *ACS Appl. Mater. Interfaces* **2015**, *7*, 11322−11329.

(6) Hu, Z.; Deibert, B. J.; Li, J. Luminescent Metal-Organic Frameworks for Chemical Sensing and Explosive Detection. *Chem. Soc. Rev.* **2014**, *43*, 5815−5840.

(7) Bünzli, J. C. G.; Eliseeva, S. V. Intriguing Aspects of Lanthanide Luminescence. *Chem. Sci.* **2013**, *4*, 1939−1949.

(8) Sanda, S.; Parshamoni, S.; Biswas, S.; Konar, S. Highly Selective Detection of Palladium and Picric Acid by a Luminescent MOF: A Dual Functional Fluorescent Sensor. *Chem. Commun.* **2015**, *51*, 6576−6579.

(9) Li, H.; Fan, J.; Hu, M.; Cheng, G.; Zhou, D.; Wu, T.; Song, F.; Sun, S.; Duan, C.; Peng, X. Highly Sensitive and Fast-Responsive Fluorescent Chemosensor for Palladium: Reversible Sensing and Visible Recovery. *Chem. - Eur. J.* **2012**, *18*, 12242.

(10) Parmar, B.; Rachuri, Y.; Bisht, K. K.; Suresh, E. Mixed-Ligand LMOF Fluorosensors for Detection of Cr(IV) Oxyanions and Fe^{3+}/Pd^{2+} Cations in Aqueous Media. *Inorg. Chem.* **2017**, *56*, 10939−10949.

(11) Doonan, C. J.; Morris, W.; Furukawa, H.; Yaghi, O. M. Isoreticular Metalation of Metal-Organic Frameworks. *J. Am. Chem. Soc.* **2009**, *131*, 9492−9493.

(12) Bloch, E. D.; Britt, D.; Lee, C.; Doonan, C. J.; Uribe-Romo, F. J.; Furukawa, H.; Long, J. R.; Yaghi, O. M. Metal Insertion in a Microporous Metal-Organic Framework Lined with 2,2'-Bipyridine. *J. Am. Chem. Soc.* **2010**, *132*, 14382−14384.

(13) Tu, T. T.; Nguyen, M. V.; Nguyen, H. L.; Yuliarto, B.; Cordova, K. E.; Demir, S. Designing Bipyridine-Functionalized Zirconium Metal-Organic Frameworks as a Platform for Clean Energy and Other Emerging Applications. *Coord. Chem. Rev.* **2018**, *364*, 33−50.

(14) He, J.; Zha, M.; Cui, J.; Zeller, M.; Hunter, A. D.; Yiu, S.-M.; Lee, S.-T.; Xu, Z. Convenient Detection of Pd(II) by a Metal-Organic Framework with Sulfur and Olefin Functions. *J. Am. Chem. Soc.* **2013**, *135*, 7807−7810.

(15) Binnemans, K. Interpretation of Eu(III) Spectra. *Coord. Chem. Rev.* **2015**, *295*, 1−45.

(16) Tang, Q.; Liu, S.; Liu, Y.; Miao, J.; Li, S.; Zhang, L.; Shi, Z.; Zheng, Z. Cation Sensing by a Luminescent Metal-Organic Framework with Multiple Lewis Basic Sites. *Inorg. Chem.* **2013**, *52*, 2799−2801.

(17) *Palladium, Environmental Healthy Criteria Series 226, International Programme on Chemistry Safety*; World Health Organization: Geneva, Switzerland, 2002.

DOI: 10.1021/acs.inorgchem.8b02871
Inorg. Chem. XXXX, XXX, XXX−XXX